Phase change materials designed from Tetra Pak waste and paraffin wax as unique thermal energy storage systems

Phase change materials designed from Tetra Pak waste and paraffin wax as unique thermal energy storage systems

Taghreed Al-Gunaid[a], Patrik Sobolčiak[a], Ibtissem Chriaa[b], Mustapha Karkri[b], Miroslav Mrlik[c], Markéta Ilčíková[c,d,e], Tomáš Sedláček[c,f] Anton Popelka[a], Igor Krupa[a,*]

[a]*Center for Advanced Materials, Qatar University, P. O. Box 2713, Doha, Qatar*

[b]*Univ Paris Est Creteil, CERTES, F-94010 Creteil, France*

[c]*Centre of Polymer Systems, Tomas Bata University in Zlin, Trida T. Bati 5678, 760 01 Zlin, Czech Republic*

[d]*Department of Physics and Materials Engineering, Faculty of Technology, Tomas Bata University in Zlin, Vavreckova 275, 70 01 Zlin, Czech Republic*

[e]*Polymer Institute, Slovak Academy of Sciences, Dubravska cesta 9, 845 41, Bratislava 45, Slovakia*

[f]*Department of Polymer Engineering, Faculty of Technology, Tomas Bata University in Zlin, Zlin, Czech Republic*

[*]*Corresponding author. E-mail address: igor.krupa@qu.edu.qa (I. Krupa).*

ABSTRACT

Thermal energy storage systems (TES) based on shape-stabilized phase change materials ($SSPCM$) designed from recycled Tetra Pak (TP) waste, paraffin wax (PW), and expanded graphite (EG) were investigated in this study. This work represents the first study to explore TP waste composed of low-density polyethylene ($LDPE$)/ aluminum (Al) components for energy storage applications. The $LDPE$ part serves as a matrix conserving a material in a compact, solid shape after PW melting; PW acts as an active phase change component contributing to heat absorption/release through a phase change (from a solid to a liquid state, and vice versa) of its crystalline phase. EG serves as a filler that enhances the thermal conductivity and mechanical properties of materials.

The focus was put on the optimization of the composition of $SSPCM$ including PW, and EG, to check thermal, mechanical, and rheological properties which influence the future processability of such systems through extrusion, as well as to investigate the synergic effect of graphite and residual Al component on thermal conductivity and leakage of PW. There are two main demands on polymer/PW blends, namely well-separated melting peaks for both components at significantly different temperatures, and good compatibility between polymer and PW.

The best performance of $SSPCM$ investigated in this study was found for a mixture having the composition $TP/\ PW/EG$ = 50/40/10 w/w/w. This mixture shows well-balanced properties, including appropriate heat storage and release parameters, thermal conductivity, thermal diffusivity, toughness and strength, and low leakage of PW from the material. This system can store 116.2 J/g of heat energy and release 93.8 J/g of heat energy. The determination of the heat energy storage and release was performed by the transient guarded hot plate technique. Tensile testing revealed that Young's

modulus of the $TP/PW/EG$ = 50/40/10 w/w/w composition was 924 $\pm$ 71 MPa and the stress at break was 8.2 ± 1.2 MPa, which are sufficient values from the applicability point of view. The composition stability of the prepared system was confirmed by rotational rheometry. The environmental relevance of these materials lies in the utilization of the waste, which has minimal usage, and after the hydropulping of Tetra Pak packaging, it accumulates in large volumes. This is the first study indicating that $LDPE/Al$ recyclate is a cheap alternative for preparing TES materials, fulfilling all the requirements for such materials. This study indicates the potential of TP waste for the preparation of $SSPCM$ using PW as a phase change component. The selection of PW with a specific melting point determines potential applications, including the building industry, thermal management of electronics, solar vapor generators for desalination, solar water heaters, battery/computer heat protection, etc.

Keywords: Tetra Pak waste, recycling, paraffin, low-density polyethylene, phase shape materials, heat absorption

1. Introduction

Tetra Pak® packaging is multi-material multilayer aseptic packaging composed mainly of low-density polyethylene, aluminum, and paperboard sheets. It comprises six layers — four $LDPE$ layers, one paper layer, and one aluminum layer, and the standard composition of paperboard/$LDPE/Al$ structures is approximately 75/20/5 wt% [**1**]. Most packaging in the food industry is a one-time used item with a short life cycle [**2**], and a majority of post-consumer items are disposed of in landfills [**3**]. Combustion and pyrolysis are standard technologies applied for relatively simple reduction of packaging volumes [**4,5**]. Porous carbon was employed as a skeleton for the incorporation of paraffin wax to prepare $SSPCM$ with reduced leakage and enhanced thermal conductivity [**6**].

Recycling routes of Tetra Pak waste, which can utilize all of the main components, are the most desirable approaches; however, the complexity of these structures makes recycling technologies challenging from both technical and economic points of view [**3**]. In general, the recycling process of Tetra Pak waste can be divided into two broad groups: i.) full package recycling without separating its components [**7**], mostly used for cardboard panels construction [**8**] and ii.) paperboard recycling or hydropulping, in which paper is separated from a polyethylene and aluminum mixture to be used for the production of cardboard, paper towels, notebooks, etc. [**9**]. The core challenge concerns the effective use of $LDPE/Al$ waste obtained after paperboard removal to transform it into marketable products. $LDPE/Al$ waste can be treated to separate individual Al and $LDPE$ components through the removal of pure Al from mixtures using plasma-assisted Al melting [**10**], a separation of $LDPE$ and Al components using both acids [**11**] and solvent-based based delamination [**12-14**] or solvent-based extraction of $LDPE$ [**15**]. However, the most limiting factor is a very low interest in convertors of plastics in recycled $LLDPE$ in general due to the impossibility of reusing $LDPE$ waste for their primary application, namely, its reprocessing as packaging materials, particularly foils [**16**]. The optimum strategy should be based on the economically viable utilization of $LDPE/Al$ structures as obtained after the hydropulping process without any specific posttreatment. The products prepared in this way include roof tiles, panels, and floors [**17**]. The main problem with these products is the same as with recycling $LDPE$ itself: the low interest in plastic convertors and the limited marketability of these commodities. The scientific focus in this area should therefore be oriented on the development of new materials (products), which should have at least two general features: i) a specific application does not require high mechanical performance and esthetic criteria, and ii) the material has a special functionality, and this functionality is not influenced using a recyclate against the use of the pristine

polymer. In the ideal case, the recyclate is even more advantageous against neat polymers in some aspects. This task is not trivial, and we propose and explore one of these possibilities in this manuscript.

The materials reported in this study, shape-stabilized phase change materials ($SSPCM$s), belong to the family of thermal energy storage (TES) materials [**18**]. TES are materials that effectively absorb and release excess thermal energy to ensure indoor thermal comfort, with minimal use of electrical energy for heating in winter and cooling in summer being a matter of high economic and ecological relevance [**19**]. These materials reduce variations in the temperature of buildings during temperature changes over a day without needing external energy sources. Phase change materials (PCMs), in general, are materials that can undergo a phase transition between the solid and liquid phases at the selected temperature while absorbing or releasing a high amount of energy, which is proportional to their specific enthalpy of melting [**20**]. Thermal energy storage belongs to the most common applications of PCM not only in the building industry but also in the thermal management of electronics (heat sinks), food protection, etc. [**21**]. Metallic structures such as copper foams and pipes represent other options for the incorporation of active phase change components into complex systems [**22**].

Paraffin waxes (PW) are the most promising due to their favorable characteristics, such as a high enthalpy of melting/crystallization, a broad range of melting temperatures dependent on the number of carbons in the paraffinic chain, high specific enthalpy of melting, chemical stability, negligible super-cooling, availability, and a relatively low price [**23**]. Due to their leakage after melting, PW must be fixed in a stable form. Direct mixing of polymers with PW is a prospective approach for that purpose that enables the incorporation of much higher PW content into a material. Different polymeric matrices can be used for this purpose; however, the most common ones are various grades of polyethylene (PE). They can reduce post-melting leakage, the extent of which is dependent on the compatibility or partial miscibility of PW and PE components. The resulting materials are referred to as shape-stabilized PCMs ($SSPCM$s). Various PE grades including low-density PE [**24**], high-density PE [**25**], and linear low-density PE [**26**] are the most frequently used polymer for blending with PW because of their chemical and structural similarity. The $SSPCM$ reported in this paper is designed from Tetra Pak waste as a matrix, PW as an effective phase change component, and expanded graphite (EG) as a filler, which particularly enhances the thermal conductivity of materials and their Young's modulus and partly reduces PW leakage [**26**]. EG also suppresses degradation behavior under light (UV) exposition [**27**].

Practical implications of these materials are determined by the melting point of PW, which is around 42 °C, and in combination with polymeric matrix (TP waste, in this case) and enhanced thermal conductivity enables manufacturing of $SSPCM$ applicable in thermal management of electronics, solar vapor generator for desalination, and solar water heaters. For example, Wen-Long et al. [**28**], and Mousa et al. [**29**] investigated the improvement of solar still performance aiming at a replacement of conventional metal absorber plates employing phase change materials. Dhinakaran et al. [**30**] explored phase change materials for an improvement of the functionality of solar water heaters. Xiaobin Gu et al. [**31**] investigated efficient solar vapor generation in both daytime and nighttime via the integration of $FSPCM$-based thermal storage technology.

2. Materials and methods

2.1. Materials

Tetra Pak (TP) waste was obtained after processing Tetra Pak cartons by hydropulping and extrusion in the form of coarse-grained particles of irregular sizes (**Fig. 1**) containing approximately 80 wt% low-

density polyethylene ($LDPE$) and 20 wt% aluminum (Al). Paraffin wax (PW; grade RT42, Rubitherm® Technologies GmbH, Germany) was used as an active phase change component.

Fig. 1. Photograph of TP waste material.

Expanded graphite (EG; Carbon's $SIGRATHERM$®, Germany), having an average lateral particle size of 200 |im was used to improve thermal conductivity and suppress PW from the final products.

2.2. Sample preparation

The $SSPCM$ mixtures were prepared by hot blending all components (TP, PW, and EG) at selected ratios in a 50-mL mixing chamber of a Brabender® Plastograph® EC W50 PLE 331 (Duisburg, Germany) for 10 min at 160 °C and a mixing speed of 35 rpm. The compositions and the specific densities of the mixtures are summarized in **Table 1**.

The samples of required shapes for different tests were prepared using a hydraulic mounting press machine (Carver 3895, USA) at a temperature of 160 °C for 3 min.

2.3. Scanning Electron Microscopy/EDS

The microstructure of the materials was examined by a field emission scanning electron microscope ($FE-SEM$, Nova Nano SEM 650) equipped with energy dispersive X-ray spectroscopy (EDS) by secondary electron imaging at 3 kV and at different magnifications. All specimens were sputter-coated with 2-nm gold before SEM.

2.4. Differential scanning calorimetry (DSC)

DSC measurements were performed using a Perkin Elmer model DSC 8500 (Perkin Elmer, USA) in a temperature range from 0 °C to 150 °C at a heating rate of 2 °C/min under a nitrogen atmosphere. The specific enthalpies of melting were calculated from the second heating curve to suppress the thermal history of the samples. Nitrogen gas was passed through the instrument at a flow rate of 20 ml/min. All measurements were repeated at least three times.

2.5. Thermogravimetric analysis (TGA)

The composition and thermal stability of the selected materials were characterized by thermogravimetric analysis (TGA) (4000 Perki-nElmer® Pyris system) in a nitrogen atmosphere. The mass of each sample was approximately 20 mg. The range of temperature in this test was from ambient room temperature (≈30 °C) to 600 ° C at a heating rate of 5 °C/min.

2.6. Measurement of thermal conductivity and thermal diffusivity

Thermal conductivity and thermal diffusivity were determined by a homemade device ($DICO$) using the periodic temperature ramp method [**32-35**]. The size of the samples was 50 × 50 × 5 mm^3.

Table 1 Compositions and specific densities of investigated composites. X/Y/Z refers to TP, PW, and EG weight percentages, respectively.[a]

Composition	TP (wt %)	PW (wt %)	EG (wt %)	Al content[a] (wt%)	Specific density ($g.cm^{-3}$)
TP	100	0	0	17.6	1.290
70/30/0	70	30	0	12.3	1.143
60/40/0	60	40	0	10.6	1.103
50/50/0	50	50	0	8.8	1.067
58/40/2	58	40	2	10.2	1.112
55/40/5	55	40	5	9.7	1.122
53/40/7	53	40	7	9.3	1.127
50/40/10	50	40	10	8.8	1.142

[a] *Al weight content in composites was calculated from Al content in TP determined by TGA (see below), which is 17.6 wt% related to TP.*

2.7. Energy storage and energy release measurement

The determination of heat energy storage and release was performed using the transient guarded hot plate technique ($TGHPT$). A parallelepiped-shaped sample (45 × 45 × 6 mm^3) was placed between two isothermal aluminum heat exchanger plates connected to thermoregulated baths, allowing the temperature of the injected oil H10 to be finely regulated with a precision of approximately 0.1 °C. Heat flux sensors from Captec company and thermocouples (type T) were placed on each side of the composite sample to measure the heat flux $\emptyset_{1,2}$ and temperature $T_{1,2}$ on each face of the composite. The lateral sides of the studied samples were insulated by polyethylene-expanded foam (PE), which creates an insulating ring around the sample and minimizes heat transfer to the external environment.

The sensors are connected to the LabVIEW program adapted to measure temperature fluctuations, and heat flux exchanged during melting and solidification processes. Experimental data were recorded at regular and adjustable time steps (1 s-6 s).

2.8. Rheological and dynamic mechanical characterizations

Rheological characterization was performed around the melting point of the TetraPak using an Anton Paar MCR 502 rotational rheometer (Anton Paar, Austria). The samples were measured at various temperatures (60 °C - 130 °C), which were controlled using a lower Peltier measuring cell (Anton Paar, Austria) and upper measuring system PP25 (Anton Paar, Austria). The samples in the form of discs 25 mm in diameter were cut from a polymer sheet of 0.5 mm thickness. All measurements were performed in the linear viscoelastic region set in the range from 0.04 % to 0.08 %, depending on the sample composition. Frequency sweep measurements were performed from 0.1 to 10 Hz, and viscoelastic moduli, G' (storage modulus) and G" (loss modulus), were recorded.

Dynamic mechanical analysis of the composite systems was performed using the same device and measuring cell as was used for rheological characterization, but the upper measuring system PP10 was applied for these measurements. The linear viscoelastic region was set to 0.02 %. In this case, the temperature sweep from 10 °C to 70 °C was investigated at 1 Hz. Demonstrating that there are no significant changes in materials' behavior during the cycles of heating/cooling, ten cycles were performed, and G' and tan delta were shown as a function of temperature.

2.9. Tensile mechanical properties

The static mechanical properties were tested in tensile mode at 22 °C and a deformation rate of 10 mm/min using a universal tensile machine (Lloyd Instruments, UK, Model: LF 1 K Plus). Dog-bone-shaped specimens of 25 mm gauge length and 3.21 mm width were cut from the slabs. Six samples were tested for each material.

2.10. Leakage test

A leakage experiment was performed to characterize the weight loss of PW from materials kept under elevated temperatures above the melting point of PW for selected periods. Thin strips of $SSPCM$ specimens with dimensions of 60 × 60 × 1 mm^3 were placed in a vertical position in an oven at 60 °C for 10 days. The samples were weighed daily to record the weight loss. Before weighing, the samples were cleaned with a cloth to remove excessive wax deposited on the surface. The weight loss of the PW component in the SSPCM specimens was calculated from Eq. (1):

$$\text{Weight loss, W } (\%) = \left(\frac{m_0 - m_x}{m_0 W}\right) \times 100 \qquad (1)$$

where m_o is the initial mass of the specimen, mx is the mass of the specimen after leakage of PW, and W is the mass fraction of paraffin wax within a material.

3. Results and discussion

3.1. Morphology of materials

The TP waste employed in this study was used in granular form, as shown in **Fig. 1**. The granules were obtained by compounding and pelletizing the original TP waste after hydropulping various TP packages. The size of the granules is on the order of 10^0-10^1 mm.

Fig. 2a shows an SEM image of the coarse-grained TP particles waste material, confirming the presence of the Al component. EDS analysis (**Fig. 2**b) identifies the C element as 76.8 wt%, O element 6.7 wt%, Al element 15.9 wt% and Ca as 0.6 wt%. The content of Al of 15.9 wt% is in good agreement with the TGA study, where approximately 18 wt% of solid residues were determined, including mostly Al pieces and a small content of solid impurities and carbonaceous char. A calcium content of 0.6 wt% was also indicated as an impurity that may have various origins. Oxygen originates from various impurities, processing additives, and residual water. EDS also visualizes a distribution of Al pieces within a mixture and its approximate size and shape. **Fig. 2**c shows the morphology of the mixture that contains 60 wt% TP and 40 wt% PW. The appropriately homogenously distributed two immiscible, separated phases are visible: one belongs to PE originating from recycled TP, and the other belongs to PW.

3.2. Thermogravimetry analysis

TGA was performed to investigate the thermal stability and degradation behavior of pristine TP and its mixtures with PW and EG (**Fig. 3**). Just one composition for each system is presented here, as other mixtures showed the same behavior. Pristine TP shows two distinguished degradation steps. This indicates the presence of additives or impurities, which start decomposition at approximately 275 °C, and degradation stops at approximately 550 °C. The weight portion of the detected residues after total decomposition was approximately 18 wt%. The residues are mainly composed of aluminum, as this value is very close to the Al content determined by EDS, but some unidentified residues may also be involved there. Pure PW degrades in a single degradation step starting at 182 °C and ending at 330 °C. Degradation of mixtures runs in two degradation steps, and it is seen that the decomposition of PW and im-purities/additives incorporated in TP and degrading in the same temperature region (approximately 300-440 °C) run in a parallel way. However, the onset of decomposition of PW itself within mixtures is shifted to higher temperatures. It was also observed that the influence of EG on the degradation behavior of materials is marginal.

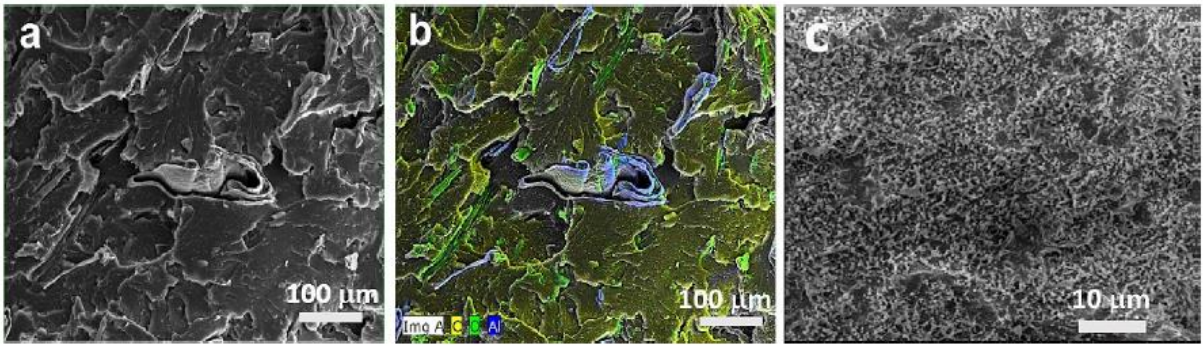

Fig. 2. a) SEM image of TP, b) EDS mapping of TP, c) TP/PW = 60/40 w/w.

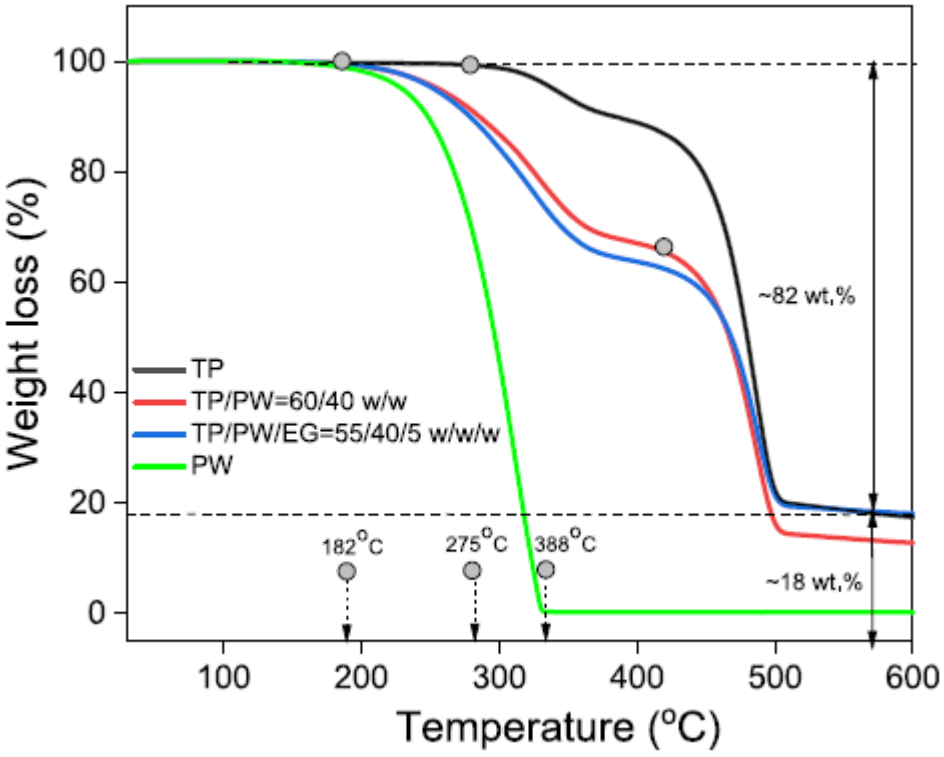

Fig. 3. TGA curves of TP and its mixtures with PW and EG.

3.3. Differential scanning calorimetry

DSC heating curves of pristine TP, PW, and their blends containing 60 wt% TP and 40 wt% PW are shown in **Fig. 4**. The composition of 60/ 40 w/w was selected for illustration because other compositions show the same behavior.

PW shows a major peak at 42 °C, characterizing the solid-liquid transition - melting of the crystalline phase of PW. This curve shows another two small peaks at 16 to 27 ° C. These peaks correspond to the solid-solid transition between various crystalline structures of PW crystallites [**36**]. Pristine TP shows two melting peaks at temperatures 107 and 126 °C, indicating that TP recyclate contains two different polyethylene grades, the one at 109 °C, which belongs to LDPE, and the second one at 125 °C, which may belong to either linear low-density polyethylene (melting point approximately 122 °C) or to $HDPE$ (melting point around 130 °C) originating from the cover lids. Composite TP/PW 60/40 shows well-distinguished peaks of TP and PW, which prove the mutual non-miscibility of TP and PW with the potential to be used as SSPCM for various energy storage applications. The heat energy is absorbed during heating in the form of sensible (given by the specific heat capacity) and latent heat, which is proportional to the specific enthalpy of melting of the active (PW) component. Suppose the temperature of the material reaches the critical value (melting point of wax - T_m). In that case, the delivered heat is consumed for the melting of PW, and the temperature of the material remains more or less constant. The material ($SSPCM$) rests in a solid, compact shape up to the onset of the polymer phase ($LDPE$ belonging to $LDPE$, in this case) melts (T_c). The amount of stored energy (heating step) and released energy (cooling step) is given by a sum of both contributions (sensible and latent heat).

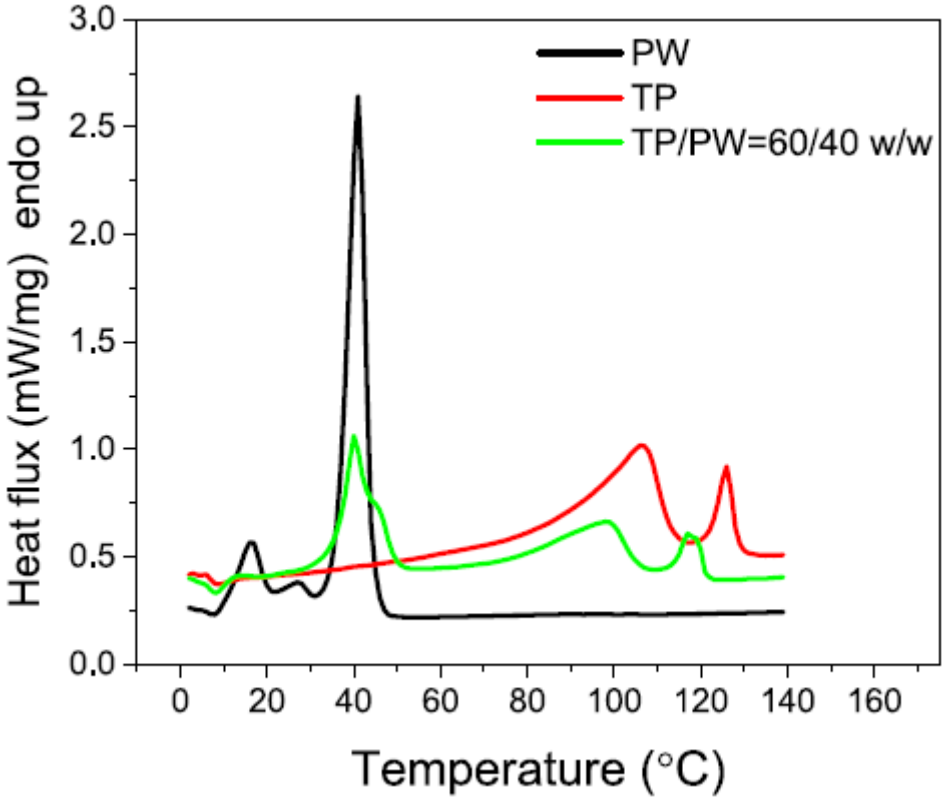

Fig. 4. Comparison of DSC heating curves of TP, PW, and TP/PW =60/40 w/w.

Most of the studies were performed in a temperature range from 0 to 60 °C to investigate the melting/solidification of PW (melting point of PW, 42 ° C) within $SSPCM$. Two peaks in the studied range were found: solid-solid transition at approximately 15 ° C and main solid-liquid transition at 42 °C. The temperatures and enthalpies for the melting and crystallization of the mixtures are summarized in **Table 2**. The enthalpies of melting enthalpy are related to the PW component increasing with an increase in the PW content. The highest value was obtained for mixtures consisting of 50 wt% PW, which equals 68.6 J/g. A decrease in melting enthalpies was observed for mixtures loaded with EG. For instance, an EG content of 10 wt% decreased the melting enthalpy of the PW component from 54.6 J/g to 44.4 J/g. This is a common phenomenon for many fillers, influencing the melting enthalpy in composites based on the semicrystalline matrix. Briefly, the melting enthalpy of any semicrystalline polymer (which is also valid for paraffin waxes, which are short-chain olefinic oligomers) depends on the amount and regularity of the folded chains. The fillers can influence both of these phenomena either positively or negatively depending on the physical and chemical character of the filler [**37**]. In our case, no regular tendency in the melting enthalpy on the filler content was observed.

3.4. Thermal conductivity and thermal diffusivity

The thermal conductivity and thermal diffusivity of the materials are summarized in **Table 3**. The study was performed at two different temperatures (below and above the melting point of PW) to compare the thermal properties of PCM in the solid and liquid states of PW within PCM blends.

Table 2 Thermal properties of composites determined by DSC. X/Y/Z refers to TP, PW, and EG weight percentages, respectively.

Composition	HEATING				COOLING			
	Ts-s (°C)	Δ Hs-s (J/g)	Ts-l (°C)	Δ Hs-l (J/g)	Ts-s (°C)	Δ Hs-s (J/g)	Ts-l (°C)	Δ Hs-l (J/g)
70/30/0	14.5 (0.4)	2.6 (0.1)	43.1 (0.4)	39.1 (0.6)	9.7 (0.4)	1.9 (0.3)	32.7 (0.4)	40.8 (0.4)
60/40/0	15.7 (0.0)	4.4 (0.2)	44.9 (0.4)	54.6 (0.8)	8.9 (0.3)	3.6 (0.4)	30.7 (0.4)	57.3 (0.9)
50/50/0	15.9 (0.5)	6.8 (0.3)	45.3 (1.4)	68.6 (0.8)	8.9 (0.8)	5.4 (0.4)	30.4 (1.6)	69.7 (0.2)
58/40/2	15.6 (0.1)	3.0 (0.0)	42.5 (0.6)	46.9 (0.4)	10.8 (0.1)	2.4 (0.6)	33.6 (0.4)	48.9 (0.1)
55/40/5	15.3 (0.4)	2.9 (0.6)	43.4 (0.4)	44.7 (0.4)	10.2 (0.1)	2.3 (0.1)	32.8 (0.4)	46.7 (0.4)
53/40/7	15.9 (0.3)	3.1 (0.8)	44.7 (0.3)	44.6 (0.6)	9.2 (0.2)	2.0 (0.1)	31.0 (0.3)	46.0 (0.6)
50/40/10	15.4 (0.2)	2.5 (0.1)	43.5 (0.2)	44.4 (0.8)	9.9 (0.1)	2.3 (0.5)	32.5 (0.0)	45.8 (1.2)

Table 3 Thermal conductivity (X) and thermal diffusivity (a) of investigated materials at 20 and 50 °C. X/Y/Z refers to TP, PW, and EG weight percentages, respectively.

Composition	Solid 20 °C		Liquid 50 °C	
	λ	α	λ	α
	(W/m.K)	(mm^2/s)	(W/m.K)	(mm^2/s)
TP	0.67	0.429	0.58	0.286
70/30/0	0.59	0.294	0.50	0.272
60/40/0	0.54	0.301	0.47	0.257
50/50/0	0.51	0.266	0.41	0.231
58/40/2	0.72	0.399	0.61	0.347
55/40/5	0.95	0.986	0.94	0.595
53/40/7	1.44	1.110	1.05	1.048
50/40/10	1.71	2.029	1.56	1.338

3.4.1. Testing at 20 °C

The thermal conductivity of recycled TP is 0.67 W/m.K. Recycled TP consists mainly of $LDPE$ and Al. The thermal conductivity of $LDPE$ is approximately 0.3 W/m.K, which depends on the degree of crystallinity of PE [**38**], whereas the thermal conductivity of Al is 237 W/m.K [**39**]. Adding PW to TP led to a small decrease in thermal conductivity because of the thermal conductivity of pristine PW, which is approximately 0.2 W/m.K. Adding 50 wt% PW caused a reduction in the thermal conductivity of the mixture to 0.51 W/m.K. One of the most common ways to increase a blend's thermal conductivity is to add a filler with high conductivity, such as graphite [**39**]. The materials, which are composed of 40 wt% PW was modified by adding various portions of EG to enhance the thermal conductivity and thermal diffusivity of the final $SSPCM$. The thermal conductivity of the $SSPCM$ blend containing 60 wt% TP and 40 wt% equals 0.54 W/m.K. Loading EG caused a noticeable increase in thermal conductivity from 0.72 W/m.K for the blend containing 2 wt% of EG to 1.71 W/m.K for the blend containing 10 wt% EG. The EG significantly improves the thermal conductivity of materials based on TP recyclate, which can be caused by an additional synergistic effect of Al flakes dispersed within materials. For comparison, the $SSPCM$ based on the $LLDPE$ matrix filled with the same grade and an EG content of 10 wt % leads to a thermal conductivity of 0.97 W/m.K only [**40**].

Similar trends were observed for the thermal diffusivity of pristine TP, which was 0.429 mm^2/s and decreased to 0.266 mm^2/s for a blend containing 50 wt% TP and 50 wt% PW. The EG enhanced thermal diffusivity to a value of 2.029 mm^2/s for mixtures containing 10 wt% EG.

3.4.2. Testing at 50 °C

In general, only minor differences were found when comparing thermal properties at 20 and 50 °C. The thermal conductivity decreased to 0.57 W/m.K for TP/PW mixtures, with a higher thermal conductivity of 1.56 W/m.K observed for a blend containing 10 wt% EG. The thermal diffusivity of TP was 0.286 mm^2/s, decreasing to 0.231 mm^2/s for a blend containing 50 wt% PW, and it reached a value of 1.338 mm^2/s for a blend containing 10 wt% EG. The decrease in thermal conductivity is caused by the melting of the crystalline phase of PW, which has a slightly higher thermal conductivity than the molten amorphous phase [**41**].

3.5. Mechanical properties

The mechanical properties do not represent the particular importance of $SSPCMs$ because they are usually not exposed to high forces during their operation life. On the other hand, materials must possess some mechanical strength and toughness to be viable for safe manipulation and use in real applications. The static mechanical properties of pristine TP and its mixtures with PW and EG obtained from standard tensile testing are listed in **Table 4**. The PW component decreases the values of all mechanical parameters in comparison to pristine TP. This is the expected behavior because soft waxes, which have low molar mass and poor mechanical properties, significantly deteriorate the mechanical properties of $LDPE$. PW acts as a plasticizer, reducing Young's modulus and the stress at break [**37**]. Moreover, the immiscibility of PW and TP also contributes to some mechanical properties' deterioration. All these parameters decrease with an increase in the wax content. EG, added into the TP/PW mixtures, enhances the Young modulus; however, the material becomes slightly more brittle. This is because filler particles suppress the deformability of the composites, as they represent defects and stress concentrators [**37**]. The influence of EG on the stress at break is marginal, and materials with and without EG show similar values of the stress at break.

3.6. Rheological and dynamic mechanical analysis

The composition stability of the prepared system regarding the influence of both PW and EG was investigated using rotational rheometry. It can be seen in **Fig. 5**a-d that the presence of PW makes the composite less stiff; this behavior is more significant at elevated temperatures. At 60 °C, G' decreases with an increasing amount of PW. The only exception is sample TP/PW 60/40, where G' is higher. However, this is a consequence of the applied higher normal force during the measurement. If the temperature is elevated to 130 °C, then pristine TP and TP with PW components within the mixture should be above their melting points, as proven by DSC. However, for neat TP, G' is still above G" but very close to each other, indicating rather solid-like than liquid-like behavior. With an increasing amount of the paraffin wax sample TP/W 70/30, the situation is different, and G" overcomes G', showing liquid-like behavior. Furthermore, the additional content of the wax decreases the absolute values of both moduli; however, the absolute change when the amount of wax is increased from 40 wt% to 50 wt% is rather insignificant, due to the good stability of the prepared systems. The values obtained at 90 °C which is the maximal expected application temperature convincingly show that all investigated samples do not change their behavior significantly, and the TP matrix holds the paraffin wax inside the system.

The influence of EG content on mechanical behavior was further investigated. In this case, the small addition of EG up to 5 wt% (**Fig. 6**a-c) still exhibits liquid-like behavior at 130 °C, showing a negligible

effect EG particles on the viscoelastic performance at such low amounts. However, if the content of EG increases to 7 wt% (**Fig. 6**d) or 10 wt% (**Fig. 6**e), G' overcomes G" in the whole measured frequency range resulting in a transition from liquid-like to solid-like behavior. This indicates that the EG stabilizes the system, similarly as was observed in a previous study [**42**].

Table 4 Mechanical properties of composites. X/Y/Z refers to TP, PW, and EG weight percentages, respectively.

Composition	Young's modulus (MPa)	Elongation at break (%)	Stress at break (MPa)
TP	1019 (84)	5.9 (2.5)	15.8 (2.2)
70/30/0	765 (65)	3.7 (1.4)	9.8 (0.9)
60/40/0	560 (61)	5.3 (2.3)	8.0 (1.1)
50/50/0	392 (29)	5.9 (2.1)	6.3 (0.9)
58/40/2	638 (42)	3.5 (1.2)	7.9 (1.0)
55/40/5	745 (48)	2.9 (0.8)	8.2 (1.1)
53/40/7	843 (52)	2.8 (0.7)	8.1 (1.3)
50/40/10	924 (71)	1.8 (0.5)	8.2 (1.2)

Finally, it can be stated, that the presence of EG particles has a positive effect on the system's compatibility and makes the composite materials based on TP and PW stiffer, which is beneficial concerning the potential applications of passive air conditioning.

The mechanical performance of the composites was evaluated to obtain information about the mechanical stability over the cycling heating/cooling in the temperature range close to the real-life applications. The monitoring of the critical parameter G' over time at temperature cycling is very important showing, how the material sustains compact and does not exhibit any significant changes. As shown in **Fig. 7**a, neat TP shows very mild changes in G' with temperature variation. Some reorganization of the material can be seen in the first cycle; however, the remaining seven cycles look very similar, showing the proper mechanical stability of the material. Furthermore, with the addition of 40 wt% PW (**Fig. 7**b), the reorganization in the first cycle occurs again; however, with further heating, the material loses mechanical performance, and G' significantly decreases. On the other hand, when the material is cooled down, the subsequent crystallization of the PW shows the system with quite good stability; however, with the lower absolute value of G' slightly less than 10^6 Pa. The material can be considered "as stable" because, over the seven following cycles, no significant changes were observed. A very similar situation was also observed for the $TP/PW/EG$ 50/40/10 sample (**Fig. 7**c). There is different visible behavior in the 1st cycle in comparison to the rest of the cycles. Here, the initial value of G' is app. 106 Pa, after the first heating and subsequent cooling cycle, the significant reorganization of the sample occurs and the presence of the EG particles contributes to the enhanced value of G' close to 10^7 Pa. Therefore, there was also clearly seen the highest difference in the mechanical properties (G' values) during the heating/cooling cycles. Due to the presence of graphite particles, the absolute value of G' is higher in comparison to both neat TP and the TP/PW composite. However, the lowest value of G' at elevated temperatures can also be caused by the higher thermal conductivity of the system and better heat exchange during the cycling procedure. Finally, it must be stated that the developed composites based on $TP/PW/EG$ show very good stability over heating/cooling cycles and show promising results from an application point of view.

3.7. Thermal storage and release performance

3.7.1. Composites without EG

The amount of total energy stored/released in thermal energy storage applications can be calculated by varying the temperature from 20 °C to 55 °C. **Fig. 8** depicts two 3-h heating/cooling cycles to allow the composite to reach thermal equilibrium. First, the composite was kept at an initial temperature T_{init} = 20 °C, which was lower than the paraffin wax's phase change point. It was then heated to T_{end} = 55 °C. Between these two isothermal states, the composite stored latent and sensible heat. It should be noted that temperature regulation necessitates a stabilization period. The sample was finally cooled to T_{init} = 20 °C. The thermal evolution from 20 °C to 55 °C allowed monitoring of the entire melting process, during which the material stored a large amount of heat. The total heat can be calculated four times using these results (twice during the storage process and twice during the release process).

Table 5 summarizes the measured stored and released heat energies of composites with varying wax contents. There was almost no difference in the amount of heat stored/released by the composites in each cycle. This result confirms the composite's stability. Thermal energy without graphite was found to decrease with increasing paraffin wax loading, as observed by Ibtissem et al. [**43**].

3.7.2. Composites with EG

Fig. 9 shows two heating/cooling cycles of 3 h to allow the composite with EG to reach its state of thermal equilibrium. The thermal evolution from 20 °C to 55 °C allowed monitoring of the complete melting proces during which the material stored a significant amount of heat. The total heat can be calculated from these results four times.

Table 6 summarizes the stored and released heat energies of the composites with different EG contents. In each cycle, there was almost no significant change in the quantity of heat stored/released by the composites. This result confirms the stability of the composite. It was observed that thermal energy increased with increasing expanded graphite loading [**44**].

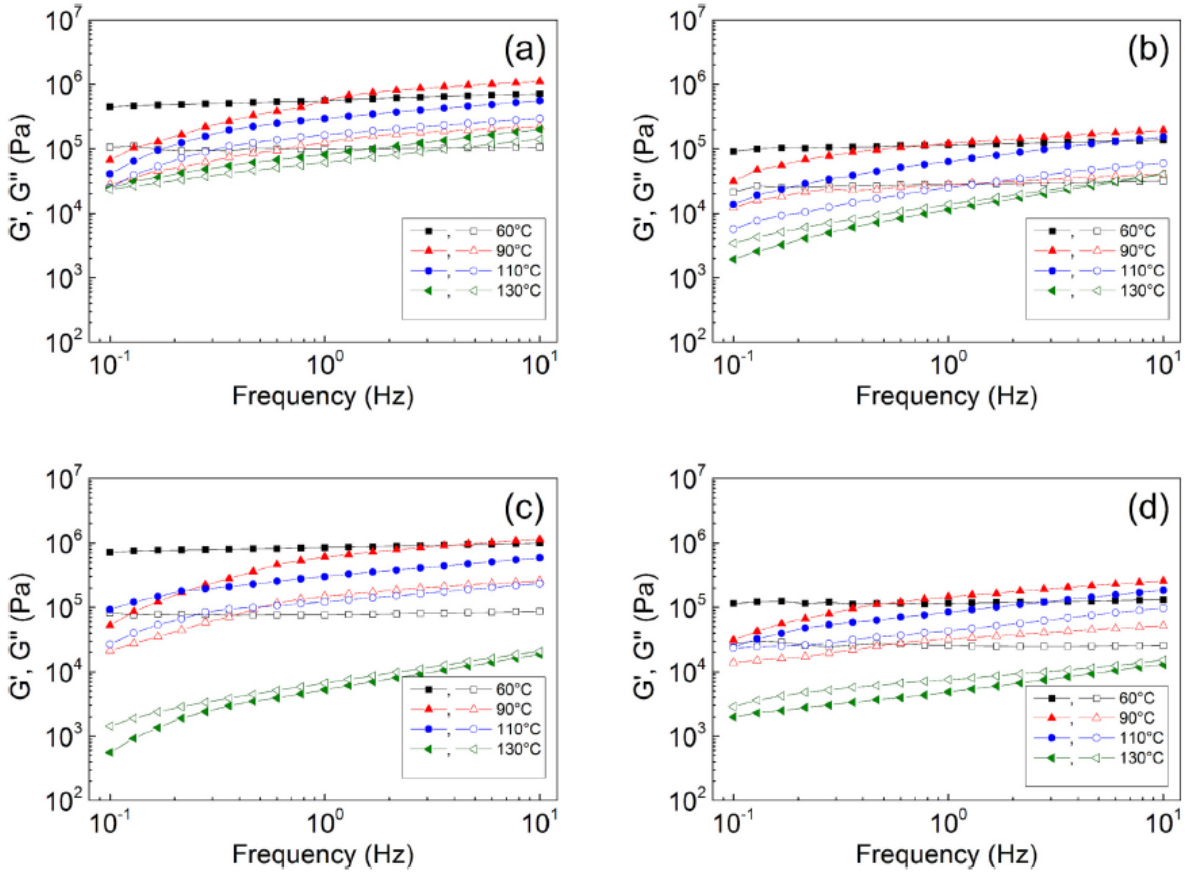

Fig. 5. Dependence of viscoelastic moduli G', storage modulus (solid symbols) and G" loss modulus (open symbols) on frequency at various temperatures for (a) neat TP, (b) TP/PW 70/30, (c) TP/PW 60/40 and (d) TP/PW 50/50.

3.8. Leakage of PW

The leakage of PW from SSPCM is a common problem that limits the practical application of these materials. Any leakage of the active PCM component (PW, in this case) causes a decrease in the storage and release capacity of the material and is also associated with potential pollution of the environment. Several approaches to suppress the leakage include encapsulation of paraffin wax, the addition of suitable filler, or surface modification of PCM blends. The leakage of PW is more pronounced with increasing PW content within the blends, as shown in **Fig. 10**. The overall leakage after ten days was approximately 6 % for an $SSPCM$ with 40 wt% PW without the incorporation of EG, which is a significantly lower value than that observed for similar PCMs using the same grade of PW and virgin PE as a matrix [**27,40**]. This is probably caused by the presence of Al flakes within the mixtures. Adding EG further reduces the extent of PW leakage, either because PW chains can penetrate between graphitic layers of EG, as reported elsewhere [**40**], and/or due to an enlargement of a diffusional path for PW chain movement. **Fig. 10** shows that the portion of leaked PW decreases with an increase in EG content, and the mixture containing 10 wt% EG lost only 2.8 % of the initial PW content after 10 days of the experiment.

Various kinds of organic and inorganic PCMs are available on the world market [**45**]; however, the commercialization of shape-stabilized PCMs, produced in the form of sheets, is very limited. We have identified just one product, called DuPont™ Energain® [**46**]. This sheet/block consists of some kind (unknown) of copolymer serving as the matrix and paraffin wax as the phase change component dispersed within the matrix. The transition between the solid and melting states (target temperature)

is approximately 18 °C, and the PW content within a system is 60 wt% with a latent heat of 70 J/g of material. No additives for an improvement of thermal conductivity are added. A thin aluminum layer additionally covers the panels to suppress the leaching of paraffin [**46**]. In the material presented in our study, the PW content is approximately 40-50 wt%, and the resulting latent heat is proportional to the specific enthalpy of PW melting.

4. Conclusions and future perspectives

Thermal energy systems based on $SSPCM$ designed from recycled Tetra Pak waste, paraffin wax and expanded graphite were investigated in this study. This work represents the first study exploring TP waste composed of polyethylene/Al components for energy storage applications. The $LDPE$ part serves as a matrix, PW acts as an active phase change component, and EG serves as a filler. The $SSPCM$ material should possess at least the following features: i) to be in a solid, compact shape after total melting of the PW component, ii.) to have sufficient heat storage capacity, iii) to have appropriately high thermal conductivity, iv) to show minimal or zero leakage of PW, v) to have satisfactory mechanical properties, and vi.) to be suitable for processing using standard plastic processing machinery. An improvement of one feature can result in the worsening of the others, so careful optimization of mixtures is needed. The best performance of $SSPCM$ investigated in this study was found for the mixture having the composition $TP/PW/EG$ = 50/40/10 w/w. This mixture shows well-balanced properties, including appropriate heat storage and release parameters, thermal conductivity, thermal diffusivity, toughness and strength, and low leakage of PW from the material. The DSC test revealed the mutual immiscibility of $LDPE$ and PW, showing two separated melting peaks at 42 °C and 100 °C belonging to PW and $LDPE$, respectively. The enthalpy of melting enthalpy related to the PW component (a latent heat) increases with an increase in the PW content. The highest value was obtained for mixtures consisting of 50 wt% PW, which equals 68.6 J/g. A decrease in melting enthalpies was observed for mixtures loaded with EG. For instance, an EG content of 10 wt% decreased the melting enthalpy of the PW component from 54.6 J/g to 44.4 J/g. The thermal energy storage, including both latent and sensible heat, was determined within the temperature range from 20 °C to 55 °C, which reflects the temperature range for real applications. Both parameters are influenced by $SSPCM$ composition. For example, the abovementioned system $TP/PW/EG$ = 50/40/10 w/w can store 116.2 J/ g of heat energy and release 93.8 J/g of heat energy. Tensile testing revealed that Young's modulus of the $TP/PW/EG$ = 50/40/10 w/w/w composition was 924 $\pm$ 71 MPa and the stress at break was 8.2 $\pm$ 1.2 MPa, which are sufficient values from the applicability point of view.

The environmental relevance of these materials lies in the utilization of the waste, which has minimal usage, and after hydropulping of Tetra Pak packaging, it accumulates in large volumes. Practically, processing $LDPE/Al$ powders or pellets is not complicated. It can be realized through the standard technologies employed in the plastic processing industry: hot compression molding, injection and rotational molding, thermoforming, and extrusion. The $LDPE/Al$ powder can be easily processed as prepared because the $LDPE$ portion in a mixture is approximately 80 wt%. This is the good content for its direct processing, or it can be modified by other components such as processing additives, additional polymers, and various fillers. The problem rests in commercial interest in such products, which do not usually have high mechanical and esthetic performance. This study indicated that $LDPE/Al$ recyclate is a cheap alternative for preparing TES materials, fulfilling all the needed requirements for such materials.

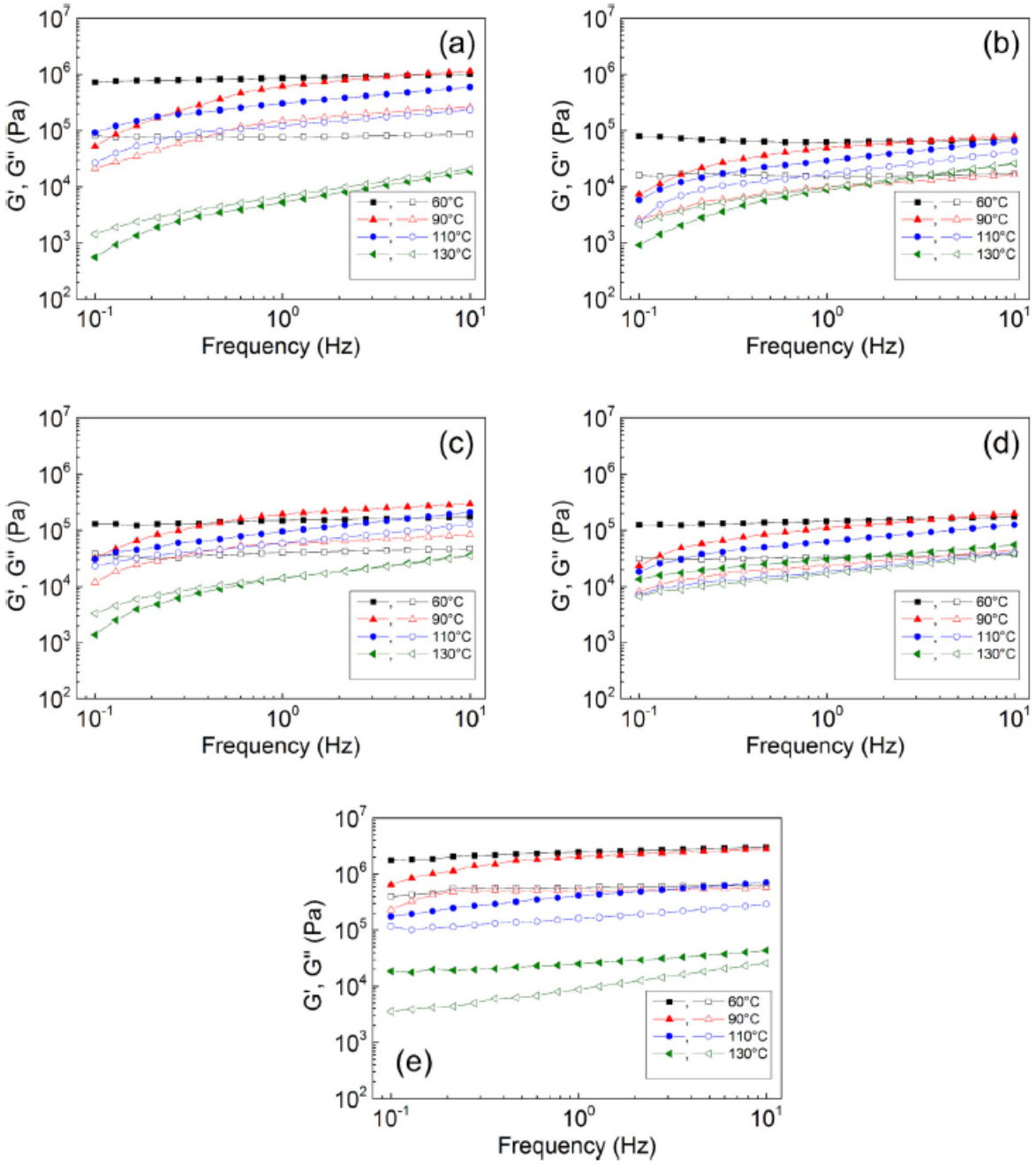

Fig. 6. Dependence of viscoelastic moduli G', storage modulus (solid symbols), and G" loss modulus (open symbols) on the frequency at various temperatures for (a) TP/PW 60/40, (b) $TP/PW/EG$ 58/40/2, (c) $TP/PW/EG$ 55/40/5, (d) $TP/PW/EG$ 53/40/7, and (e) $TP/PW/EG$ 50/40/10.

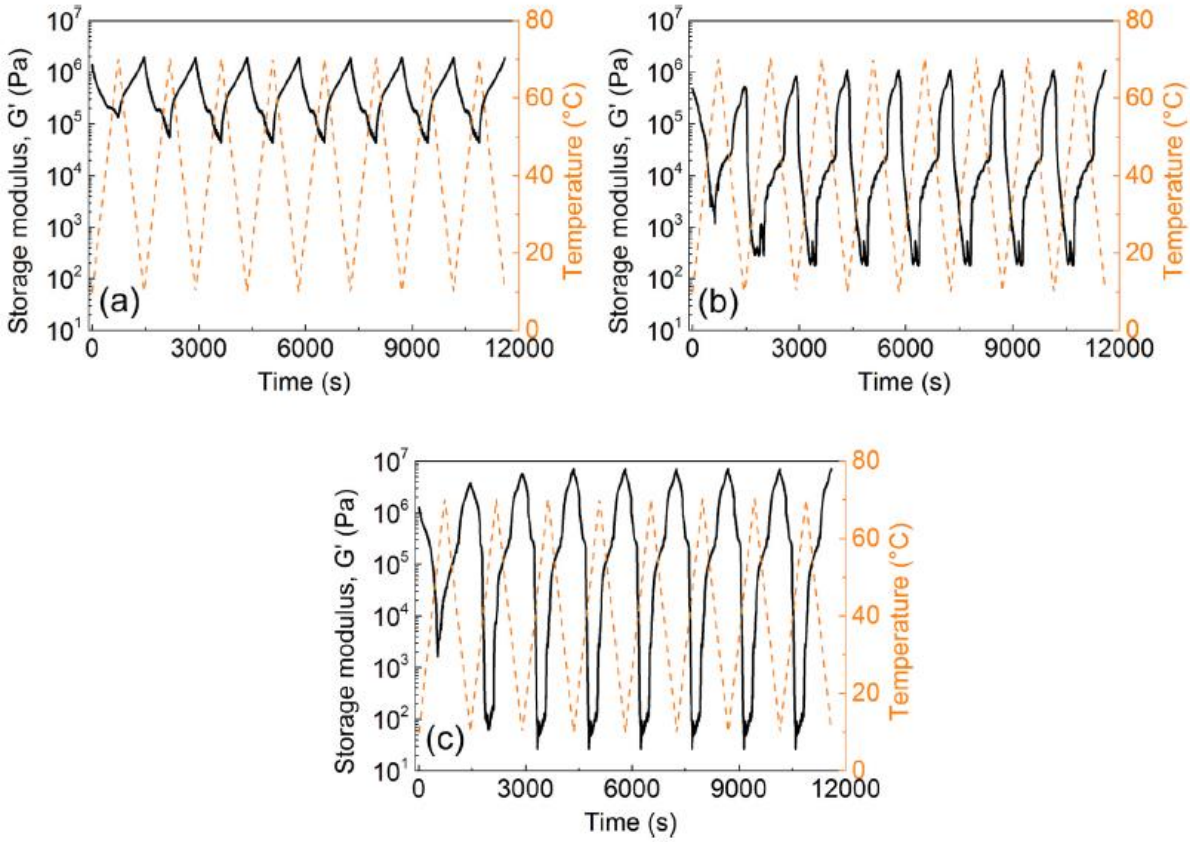

Fig. 7. Dependence of viscoelastic modulus G' and storage modulus (solid black line) on time at temperature ramp from 10 °C to 70 °C (orange dashed line) for (a) neat TP, (b) TP/PW 60/40, and (c) $TP/PW/EG$ 50/40/10.

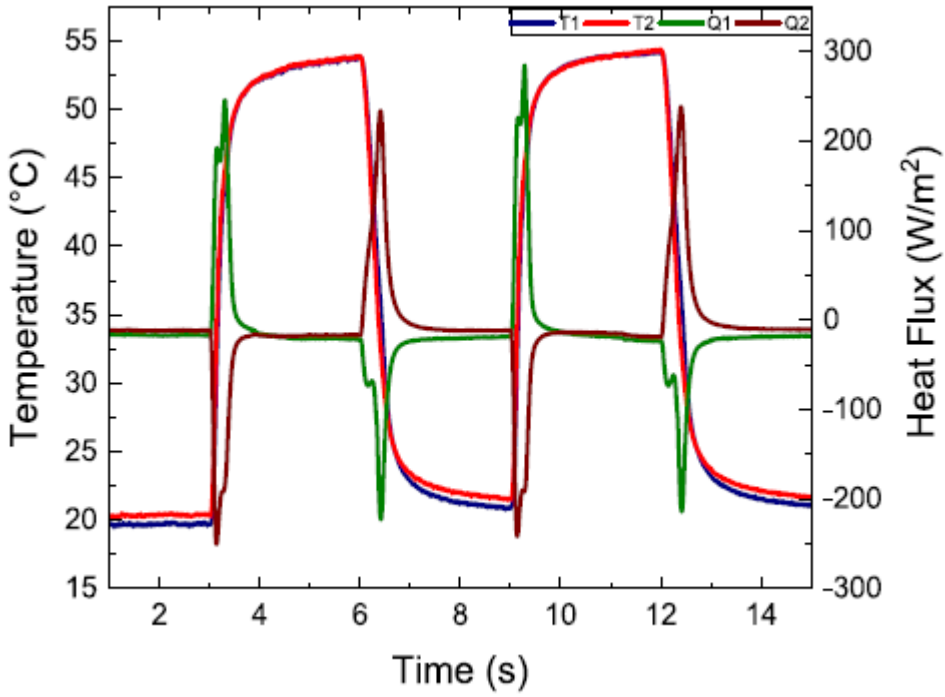

Fig. 8. Successive ramps of selected temperature ($TP/PW/EG$ = 50/50/0).

Table 5 Amount of energy stored and released in each cycle. X/Y/Z refers to TP, PW, and EG weight percentages, respectively.

Composition	Cycles	Stored energy (J/g)	Released energy (J/g)
70/30/0	1	83.77	76.38
	2	80.10	75.10
60/40/0	1	101.05	79.70
	2	98.87	79.25
50/50/0	1	118.37	93.98
	2	116.55	89.52

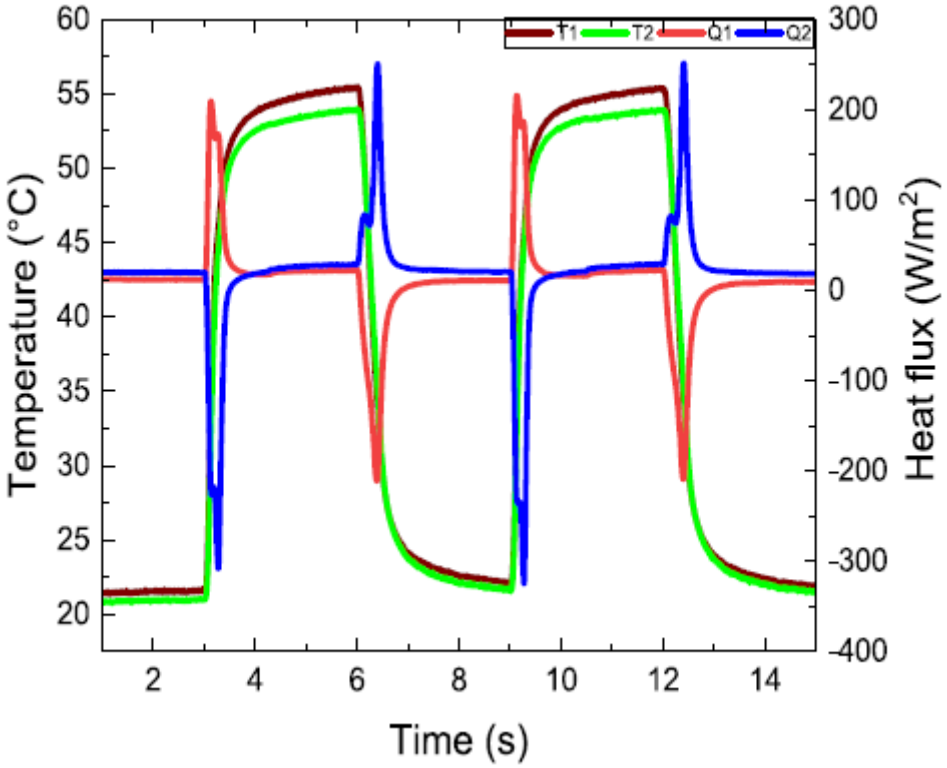

Fig. 9. Successive ramps of selected temperature ($TP/PW/EG$ = 50/40/10).

Table 6 Amount of energy stored and released in each cycle. X/Y/Z refers to TP, PW, and EG weight percentages, respectively.

Composition	Cycles	Stored energy (J/g)	Released energy (J/g)
60/40/0	1	101.05	79.70
	2	98.87	79.25
58/40/2	1	113.23	86.00
	2	113.03	86.04
55/40/5	1	113.62	93.85
	2	113.34	92.01
53/40/7	1	116.27	93.34
	2	116.09	93.16
50/40/10	1	116.31	93.94
	2	116.18	93.75

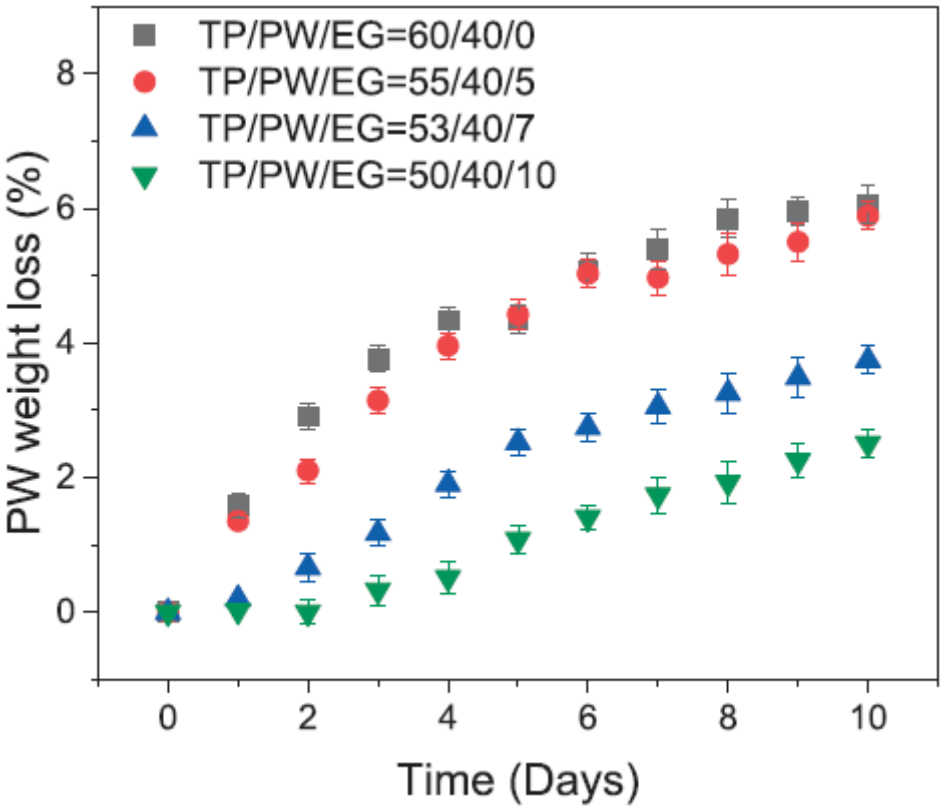

Fig. 10. Leaching of PW from selected $SSPCM$.

References

[1] S.K. Panda, J. Kellershohn, I. Russell, Probiotic Beverages, Academic Press (2021), **https://doi.org/10.1016/C2018-0-04171-7**.

[2] G.G. Sahin, M. Karaboyaci, Process and machinery design for the recycling of Tetra Pak components, J. Clean. Prod. 323 (2021), 129186, **https://doi.org/10.1016/j. jclepro.2021.129186**.

[3] C.T. de M. Soares, M. Ek, E. Ostmark, M. Gallstedt, S. Karlsson, Recycling of multimaterial multilayer plastic packaging: current trends and future scenarios, Resour. Conserv. Recycl. 176 (2022), 105905, **https://doi.org/10.1016/). resconrec.2021.105905**.

[4] M.J. Munoz-Batista, G. Blazquez, J.F. Franco, M. Calero, M.A. Martin-Lara, Recovery, separation and production of fuel, plastic and aluminum from the tetra PAK waste to hydrothermal and pyrolysis processes, Waste Manag. 137 (2022) 179-189, **https://doi.org/10.1016/j.wasman.2021.11.007**.

[5] J. Haydary, D. Susa, J. DudaS, Pyrolysis of aseptic packages (tetrapak) in a laboratory screw type reactor and secondary thermal/catalytic tar decomposition, Waste Manag. 33 (2013) 1136-1141, **https://doi.org/10.1016/). wasman.2013.01.031**.

[6] Y. Zhang, J. Wang, X. Yang, H.M. Ali, Z. Said, C. Liu, Fabrication of shape-stabilized phase change materials based on waste plastics for energy storage, J. Energy Storage. 52 (2022), 104973, **https://doi.org/10.1016/j.est.2022.104973**.

[7] A.H. Hassanin, Z. Candan, Novel bio-based composites panels from TetraPak waste, Key Eng. Mater. 689 (2016) 138-142, **https://doi.org/10.4028/www.scientific. net/KEM.689.138**.

[8] N. Ayrilmis, Z. Candan, S. Hiziroglu, Physical and mechanical properties of cardboard panels made from used beverage carton with veneer overlay, Mater. Des. 29 (2008) 1897-1903, **https://doi.org/10.1016/j.matdes.2008.04.030**.

[9] C.M.A. Lopes, M.I. Felisberti, Composite of low-density polyethylene and aluminum obtained from the recycling of postconsumer aseptic packaging, J. Appl. Polym. Sci. 101 (2006) 3183-3191, **https://doi.org/10.1002/app.23406**.

[10] J. Zawadiak, Tetra pak recycling - current trends and new developments, Am. J. Chem. Eng. 5 (2017) 37, **https://doi.org/10.11648/j.ajche.20170503.12**.

[11] D. Yan, Z. Peng, Y. Liu, L. Li, Q. Huang, M. Xie, Q. Wang, Optimizing and developing a continuous separation system for the wet process separation of aluminum and polyethylene in aseptic composite packaging waste, Waste Manag. 35 (2015) 21-28, **https://doi.org/10.1016/j.wasman.2014.10.008**.

[12] M. Xie, W. Bai, L. Bai, X. Sun, Q. Lu, D. Yan, Q. Qiao, Life cycle assessment of the recycling of Al-PE (a laminated foil made from polyethylene and aluminum foil) composite packaging waste, J. Clean. Prod. 112 (2016) 4430-4434, **https://doi. org/10.1016/j.jclepro.2015.08.067**.

[13] S.F. Zhang, L.L. Zhang, K. Luo, Z.X. Sun, X.X. Mei, Separation properties of aluminium-plastic laminates in post-consumer tetra pak with mixed organic solvent, Waste Manag. Res. 32 (2014) 317-322, **https://doi.org/10.1177/ 0734242X14525823**.

[14] I. Vollmer, M.J.F. Jenks, M.C.P. Roelands, R.J. White, T. van Harmelen, P. de Wild, G.P. van der Laan, F. Meirer, J.T.F. Keurentjes, B.M. Weckhuysen, Beyond mechanical recycling: giving new life to plastic waste, Angew. Chemie - Int. Ed. 59 (2020) 15402-15423, **https://doi.org/10.1002/anie.201915651**.

[15] T. Anukiruthika, P. Sethupathy, A. Wilson, K. Kashampur, J.A. Moses, C. Anandharamakrishnan, Multilayer packaging: advances in preparation techniques and emerging food applications, Compr. Rev. Food Sci. Food Saf. 19 (2020) 1156-1186, **https://doi.org/10.1111/1541-4337.12556**.

[16] T.W. Walker, N. Frelka, Z. Shen, A.K. Chew, J. Banick, S. Grey, M.S. Kim, J. A. Dumesic, R.C. Van Lehn, G.W. Huber, Recycling of multilayer plastic packaging materials by solvent-targeted recovery and precipitation, Sci. Adv. 6 (2020), **https://doi.org/10.1126/sciadv.aba7599**.

[17] M. Hidalgo, Manufacturing rigid board by packaging waste containing aluminum and polyethylene, J. Sci. Ind. Res. (India) 70 (2011) 232-234.

[18] V.V. Tyagi, K. Chopra, R.K. Sharma, A.K. Pandey, S.K. Tyagi, M.S. Ahmad, A. Sari, R. Kothari, A comprehensive review on phase change materials for heat storage applications: development, characterization, thermal and chemical stability, Sol. Energy Mater. Sol. Cells 234 (2022), 111392, **https://doi.org/10.1016/j. solmat.2021.111392**.

[19] F. Hassan, F. Jamil, A. Hussain, H.M. Ali, M.M. Janjua, S. Khushnood, M. Farhan, K. Altaf, Z. Said, C. Li, Recent advancements in latent heat phase change materials and their applications for thermal energy storage and buildings: a state of the art review, Sustain. Energy Technol. Assess. 49 (2022), 101646, **https://doi.org/ 10.1016/j.seta.2021.101646**.

[20] B. Zalba, J.M. Marin, L.F. Cabeza, H. Mehling, Review on thermal energy storage with phase change: materials, heat transfer analysis and applications, Appl. Therm. Eng. 23 (2003) 251-283, **https://doi.org/10.1016/S1359-4311(02)00192-8**.

[21] R.A. Lawag, H.M. Ali, Phase change materials for thermal management and energy storage: a review, J. Energy Storage. 55 (2022), 105602, **https://doi.org/10.1016/ j.est.2022.105602**.

[22] H.M. Ali, An experimental study for thermal management using hybrid heat sinks based on organic phase change material, copper foam and heat pipe, J. Energy Storage 53 (2022), 105185, **https://doi.org/10.1016ZJ.EST.2022.105185**.

[23] M. Kenisarin, K. Mahkamov, Solar energy storage using phase change materials, Renew. Sust. Energ. Rev. 11 (2007) 1913-1965, **https://doi.org/10.1016/j. rser.2006.05.005**.

[24] I. Krupa, G. Mikovaa, A.S. Luyt, Phase change materials based on low-density polyethylene/paraffin wax blends, Eur. Polym. J. 43 (2007) 4695-4705, **https:// doi.org/10.1016/j.eurpolymj.2007.08.022**.

[25] F. Cheng, Y. Xu, Z. Lv, Z. Huang, M. Fang, Y. Liu, X. Wu, X. Min, Form-stable and tough paraffin-Al2O3/high density polyethylene composites as environment-friendly thermal energy storage materials: preparation, characterization and analysis, J. Therm. Anal. Calorim. 146 (2021) 2089-2099, **https://doi.org/ 10.1007/s10973-020-10450-2**.

[26] P. Sobolciak, M. Karkri, M.A. Al-Maadeed, I. Krupa, Thermal characterization of phase change materials based on linear low-density polyethylene, paraffin wax and expanded graphite, Renew. Energy 88 (2016) 372-382, **https://doi.org/10.1016/j. renene.2015.11.056**.

[27] P. Sobolciak, H. Abdelrazeq M. Ouederni, M. Karkri, M.A. Al-Maadeed, I. Krupa, The stabilizing effect of expanded graphite on the artificial aging of shape stabilized phase change materials, Polym. Test. 46 (2015) 65-71, **https://doi.org/ 10.1016/j.polymertesting.2015.06.017**.

[28] W.L. Cheng, Y.K. Huo, Y. Le Nian, Performance of solar still using shape-stabilized PCM: experimental and theoretical investigation, Desalination 455 (2019) 89-99, **https://doi.org/10.10Wj.desal.2019.01.007**.

[29] H. Mousa, J. Naser, A.M. Gujarathi, S. Al-Sawafi, Experimental study and analysis of solar still desalination using phase change materials, J. Energy Storage 26 (2019), 100959, **https://doi.org/10.10Wj.est.2019.100959**.

[30] R. Dhinakaran, R. Muraliraja, R. Elansezhian, S. Baskar, S. Satish, V. S. Shaisundaram, Utilization of solar resource using phase change material assisted solar water heater and the influence of nano filler, Mater. Today Proc. 37 (2020) 1281-1285, **https://doi.org/10.10Wj.matpr.2020.06.460**.

[31] X. Gu, K. Dong, L. Peng, L. Bian, Q. Sun, W. Luo, B. Zhang, Round-the-clock interfacial solar vapor generator enabled by form-stable phase change materials with enhanced photothermal conversion capacity, Energy Convers. Manag. 277 (2023), 116634, **https://doi.org/10.10Wj.enconman.2022.116634**.

[32] A. Trigui, M. Karkri, C. Boudaya, Y. Candau, L. Ibos, Development and characterization of composite phase change material: thermal conductivity and latent heat thermal energy storage, Compos. Part B Eng. 49 (2013) 22-35, **https:// doi.org/10.1016/j.compositesb.2013.01.007**.

[33] A. Trigui, M. Karkri, I. Krupa, Thermal conductivity and latent heat thermal energy storage properties of LDPE/wax as a shape-stabilized composite phase change material, Energy Convers. Manag. 77 (2014) 586-596, **https://doi.org/10.1016/). enconman.2013.09.034**.

[34] M. Aadmi, M. Karkri, M. El Hammouti, Heat transfer characteristics of thermal energy storage of a composite phase change materials: numerical and experimental investigations, Energy 72 (2014) 381-392, **https://doi.org/10.1016/j. energy.2014.05.050**.

[35] A. Fethi, L. Mohamed, K. Mustapha, B. Ameurtarek, B.N. Sassi, Investigation of a graphite/paraffin phase change composite, Int. J. Therm. Sci. 88 (2015) 128-135, **https://doi.Org/10.1016/j.ijthermalsci.2014.09.008**.

[36] A. Genovese, G. Amarasinghe, M. Glewis, D. Mainwaring, R.A. Shanks, Crystallisation, melting, recrystallisation and polymorphism of n-eicosane for application as a phase change material, Thermochim. Acta 443 (2006) 235-244, **https://doi.org/10.1016Zj.tca.2006.02.008**.

[37] J.A. Manson, L.H. Sperling, Polymer Blends and Composites, Springer, US, 1976, **https://doi.org/10.1007/978-1-4615-1761-0**.

[38] G. Wypych, Handbook of Polymers, Second Edition, Elsevier Inc., 2016, **https:// doi.org/10.1016/C2015-0-01462-9**.

[39] R. Rothon, Fillers for Polymer Applications, 2017, **https://doi.org/10.1007/978-3-319-28117-9**.

[40] I. Krupa, Z. Nogellova, Z. Spitalsky, M. Malikova, P. Sobolciak, H.W. Abdelrazeq, M. Ouederni, M. Karkri, I. Janigova, M.A.S.A. Al-Maadeed, Positive influence of expanded graphite on the physical behavior of phase change materials based on linear low-density polyethylene and paraffin wax, Thermochim. Acta 614 (2015) 218-225, **https://doi.org/10.10Wj.tca.2015.06.028**.

[41] E.H.I., E.A.G.J. Brandrup, Polymer Handbook 2 Volumes Set, 4th ed., John Wiley & Sons, Inc, 1999.

[42] P. Sobolciak, M. Mrlik, M.A. Almaadeed, I. Krupa, Calorimetric and dynamic mechanical behavior of phase change materials based on paraffin wax supported by expanded graphite, Thermochim. Acta 617 (2015) 111-119, **https://doi.org/ 10.1016/j.tca.2015.08.026**.

[43] I. Chriaa, A. Trigui, M. Karkri, I. Jedidi, M. Abdelmouleh, C. Boudaya, Thermal properties of shape-stabilized phase change materials based on low density polyethylene, hexadecane and SEBS for thermal energy storage, Appl. Therm. Eng. 171 (2020), 115072, **https://doi.org/10.10Wj.applthermaleng.2020.115072**.

[44] I. Chriaa, M. Karkri, A. Trigui, I. Jedidi, M. Abdelmouleh, C. Boudaya, The performances of expanded graphite on the phase change materials composites for thermal energy storage, Polymer (Guildf). 212 (2021), 123128, **https://doi.org/ 10.1016/j.polymer.2020.123128**.

[45] S.E. Kalnæs, B.P. Jelle, Phase change materials and products for building applications: a state-of-the-art review and future research opportunities, Energy Build. 94 (2015) 150-176, **https://doi.org/10.10Wj.enbuild.2015.02.023**.

[46] Jacques Gilbert, U. Koster, Phase change materials: new thermal mass solution for low inertia buildings, in: DuPont TM Energain®, 2010, pp. 2-20.